3D Evaluation of Myocardial Systolic Wall Stress From Cardiac Magnetic Resonance Cine Data

Marion Sénési[1,2], Carine Defrance[3], Emilie Bollache[1], Ludivine Perdrix[3], Elie Mousseaux[1,3], Nadjia Kachenoura[1]

[1]INSERM U678, UPMC Univ Paris 6, Paris, France
[2]ETH Zürich, Zürich, Switzerland
[3]European Hospital Georges Pompidou, Radiology Department, Paris, France

Abstract

The aim of our study was to develop a 3D model for myocardial wall stress (MWS) evaluation and to test its ability to characterize left ventricular (LV) aging and the effect of aortic valve stenosis (AVS). We studied 65 subjects (45 controls and 20 with AVS) who had a cardiac magnetic resonance (CMR) exam and a measure of central pressures. 3D MWS evaluation combined systolic pressures and an LV geometrical factor. 3D evaluation corrected the 2D erroneous underestimation of the apical MWS. The 3D LV geometrical factor significantly decreased with aging, resulting in a normalization of the MWS which indicated the normal adaptation of the LV. Besides, the 3D MWS significantly increased in subjects with severe AVS when compared to the aged controls, reflecting an elevated afterload while it remained unchanged in subjects with less severe AVS. The addition of MWS evaluation to clinical CMR tools would enable a better characterization of LV remodeling.

1. Introduction

The left ventricular (LV) arterial coupling is a determinant factor of cardiac performance [1]. Vascular alterations, potentially accelerated by aging and other cardiovascular risk factors, lead to arterial stiffness and progressively to an increase in central mean and pulse pressures, that affects the LV. Accordingly, an effective LV-arterial coupling is strongly conditioned by the ability of the LV to adapt to an unceasingly increased arterial load by a concentric remodeling and myocardial hypertrophy if necessary. This ventricular adaptation may lead to heart failure because of the persistent and unbalanced increase in cardiac work and oxygen demand [2]. Thus, affected LV-arterial coupling may be an important predictor of heart failure. Previous studies have investigated such coupling using invasive techniques, indicating a relationship between the myocardial stiffness and the arterial load [2].

Magnetic resonance imaging (MRI) and applanation tonometry provide non-invasive, accurate and reproducible functional LV and aortic parameters. In our study, these two modalities were used to evaluate systolic myocardial wall stress (MWS), which combines the LV geometry with the downstream arterial load. This resulted in a quantitative measure of the afterload, which is known to be a major determinant of LV remodeling. Estimation of MWS has been previously performed in several studies. However, these evaluations were based on the echocardiographic or the MRI measurement of the LV geometry, combined with either invasive pressure measurements or an approximate brachial pressures assessment. Moreover, in previous clinical studies, MWS was mostly evaluated on single LV slices.

Accordingly, based on the excellent spatial and temporal resolutions as well as the LV coverage of short-axis MR data, and the accurate measurement of central pressures by applanation tonometry of one carotid artery, a model for 3D MWS evaluation was developed and compared against an in-plane 2D approach. Furthermore, the ability of the 3D MWS to characterize the effect of aging and aortic valve stenosis (AVS) on LV remodeling was investigated on healthy volunteers (aged between 18 and 81 years) and patients with calcified AVS.

2. Methods

2.1. Study population

A group of 45 controls, free from overt cardiovascular disease, and a group of 20 patients with a calcified AVS

were studied. The group of controls was divided into two subgroups C1 and C2 according to their age. C1 group included 23 controls (13 men, age: 26 ± 5 years) and C2 group included 22 controls (13 men, age: 55 ± 9 years). The group of patients with AVS was divided into two subgroups AVS1 and AVS2 according to their aortic valve area normalized by the body surface area (AVA-BSA). AVS1 group included 8 patients (4 men, age: 72 ± 13 years) with AVA-BSA > 0.45 cm^2/m^2 and AVS2 group included 12 patients (9 men, age: 82 ± 11 years) with AVA-BSA < 0.45 cm^2/m^2.

2.2. Data acquisition

All subjects had: 1) MRI exam performed on a GE 1.5 T magnet (GE Healthcare, Milwaukee, Wisconsin, USA). First, a scout view was used to localize the heart axis. The images acquisition was then aligned on the identified axes and several short axis slices (12 to 14 slices) were acquired for each subject, using a cardiac phased-array coil and an ECG-gated Cine steady-state free-precession (SSFP) sequence with the following acquisition parameters: TR = 3.6 ms, TE = 1.6 ms, flip angle = 50°, acquisition matrix = 224x190, slice thickness = 8 mm, pixel spacing = 0.74 mm, inter-slice gap = 1 mm. Of note, brachial pressures were measured simultaneously to the MR acquisition using a sensor cuff (Vital Signs Monitor, Welch Allyn Inc, USA). 2) Applanation tonometric exam was performed using the Pulse Pen device (Diatecne, Milano, Italy), immediately after the MR acquisition, to measure carotid-femoral pressures. 3) Doppler echocardiography (Vivid 7, GE Healthcare, Wauwatosa, Wisconsin, USA), which was performed the same day as the MRI exam. The blood flow velocities through aortic valve were recorded.

2.3. Pressure measurements

Because carotid pressures reflect the central pressures better than brachial pressures, we used tonometric measurements rather than brachial measurements, as commonly performed for wall stress assessment. Indeed, data from invasive studies showed that using carotid artery pressures as central pressures may only slightly overestimate the pulse pressure in the ascending aorta with less than 2 mmHg [3]. However, because our tonometric measurements were performed outside the magnet, a calibration of the blood pressure was required. This calibration was based on the fact that the mean blood pressure and diastolic pressure are nearly constant throughout the large artery tree [4]. Thus, the continuous measurement of the carotid pressure was scaled and realigned using the brachial diastolic and mean pressure values assessed simultaneously to the MR acquisition.

During the ejection phase in healthy subjects, the pressure is assumed to be homogeneous within the LV and the aorta. However, for patients with AS, the valve opening is only partial, resulting in a pressure gradient across the valve during the ejection [4]. This pressure gradient was added to the peak central tonometric systolic pressure to derive the LV peak systolic pressure (PSP). It was calculated using the simplified Bernouilli equation from the trans-aortic blood velocities provided by Doppler echocardiographic acquisitions.

2.4. Wall stress evaluation

For each subject, basal slices with a visible deformation in the myocardium due to the outflow tract were excluded. For the remaining slices, endocardial and epicardial contours were manually drawn by an experienced cardiologist on both end-systolic and end-diastolic images.

Grossman et al. [5] developed an approximate mechanical model to assess the MWS. The model was based on a simplified geometry with concentric spherical or ellipsoidal representations of the myocardium. Using the equilibrium between the pressure load inside the LV cavity and the tension across the myocardial wall, the longitudinal stress was expressed as follows:

$$MWS = P.GF, \qquad GF = \frac{R}{2.T(1+\frac{T}{2.R})} \qquad (1)$$

where P is the LV PSP and GF is the LV geometrical factor. R is the endocardial radius and T is the myocardial thickness.

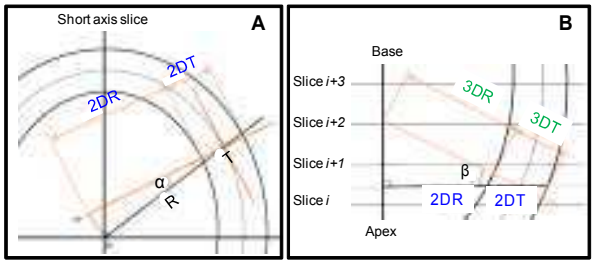

Figure 1. A: Definition of the angle α used for the 2D correction of the myocardial thickness (T) and the endocardial radius (R). B: Definition of the angle β used for the 3D correction.

The myocardial thickness was locally calculated considering the cords between the endocardial and the epicardial contours perpendicular to the centerline. This provided a locally corrected myocardial thickness in agreement with the known centerline approach. Figure 1.A shows the definition of the angle α, which enabled the estimation of the 2D corrected thickness (2DT) and radius (2DR) according to the following formula:

$$2DT = T.\cos\alpha \qquad 2DR = \frac{R+\frac{T}{2}}{\cos\alpha} - \frac{2DT}{2}$$

The corrected myocardial thickness and cavity radius were replaced in the equation (1) to calculate the 2D MWS.

Because of the ovoid shape of the LV, especially in the apical region, an accurate approximation of the myocardial thickness can be defined perpendicularly to the longitudinal centerline of the myocardium. To calculate the 3D corrected myocardial wall thickness (3DT) and radius (3DR), the approach used in the radial direction for the 2D correction was adapted to the longitudinal direction. The longitudinal centerline was defined from the previously described short axis centerlines. Then, similar to the above estimation of the angle α, the angle β was defined as illustrated in figure 1.B and used for the 3D correction of the thickness and radius, according to the following formula:

$$3DT = 2DT.\cos\beta \qquad 3DR = \frac{2DR + \frac{2DT}{2}}{cos\ \beta} - \frac{3DT}{2}$$

The angle of curvature, β, was calculated between each couple of adjacent slices from apex to base and used to correct the 2D radius and thickness of the slice located towards the apex. Thus, the 3D correction of the most basal slice was not possible, resulting in a number of slices for the 3D model equal to the total number of slices in the dataset minus one.

2.5. Statistical analysis

Mean values and standard deviations of the LV functional parameters were calculated. Non parametric statistical test (Mann-Whitney) was used to compare LV function parameters obtained in the different populations. A p value < 0.05 indicated statistical significance.

3. Results

3.1. Effect of the 3D correction

Figure 2 shows mean values and standard deviations of 2D MWS and 3D MWS calculated on the extreme apical and basal slices of the 45 healthy volunteers. The 3D correction reduced the erroneous apex-base gradient in MWS. Thus only 3D MWS is presented in the following analyses.

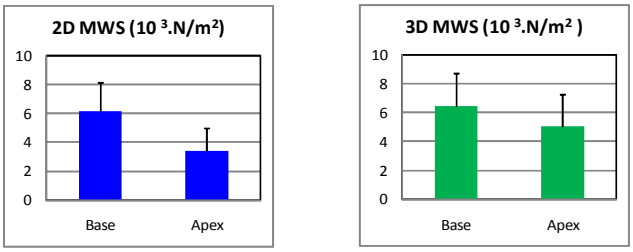

Figure 2. Effect of the 3D correction.

3.2. Effect of aging

Table 1 summarizes mean values and standard deviations of central peak systolic pressures, remodeling parameters and 3D MWS calculated for the two subgroups of controls C1 and C2. Among the LV remodeling parameters, the known ratios combining LV mass (LVM) and end-systolic (ESV) or end-diastolic (EDV) volumes, as well as our 3D LV geometrical factor (3D GF), were calculated from MRI data. Only our 3D geometrical factor was able to characterize aging. Indeed, this parameter significantly decreased with aging as a response to the significantly elevated pressure. This adaptation of LV geometry to the increased load resulted in the normalization of the MWS with aging.

Table 1. Central peak systolic pressures (PSP), remodeling parameters and 3D MWS for the subgroups of controls C1 and C2.

	C1	C2	p value
Age (years)	26±5	55±9	
PSP (mmHg)	100±12	110±13	0.03
LVM/ESV (g/ml)	2.6±0.8	3.1±1.1	0.06
LVM/EDV (g/ml)	0.92±0.18	1.04±0.30	0.22
3D GF	65±20	42±19	0.0005
3D MWS (10^3.N/m^2)	6.5±1.9	5.4±2	0.08
EF (%)	64±5	66±7	0.18

3.3. Effect of aortic valve stenosis

Table 2 summarizes mean values and standard deviations of central peak systolic pressures, remodeling parameters and 3D MWS calculated for the two subgroups of patients with aortic valve stenosis AVS1 and AVS2.

Table 2. Central peak systolic pressures (PSP), remodeling parameters and 3D MWS for the subgroups of patients with aortic valve stenosis AVS1 and AVS2.

	AVS1	AVS2
AVA-BSA (cm^2/m^2)	0.52±0.08	0.35±0.07
PSP (mmHg)	202±9	201±28
LVM/ESV (g/ml)	5.6±2.7	4.2±2.4
LVM/EDV (g/ml)	1.67±0.65	1.49±0.29
3D GF	27±17	45±26
3D MWS (10^3.N/m^2)	5.4±3.2	8.7±4.4
EF (%)	69±13	60±13

Comparison of values obtained in the AVS1 group against those obtained in the C2 group resulted in significant differences for PSP, LVM/ESV, LVM/EDV and 3D GF. These significant differences indicated an additional LV remodeling in response to the substantially elevated PSP, which induced the normalisation of MWS.

Comparison of values obtained in the AVS2 group against those obtained in the C2 group indicated a significant elevation of LV pressures. However, the parameters of LV remodeling remained unchanged, indicating the inability of the LV to adapt to the increased load. This was reflected by a significant increase of MWS in the AVS2 group. Of note, the majority (8/12) of patients in the AVS2 group had myocardial fibrosis on the MR delayed enhancement images.

4. Discussion

In this study, a 3D model for the estimation of the MWS was implemented and tested on a group of healthy volunteers, aged between 18 and 81 years, and a group of patients with different degrees of AVS. In contrast with previous studies, our MWS evaluation combined CMR and applanation tonometry, which are considered as the clinical references respectively for the evaluation of the global LV function and the measurement of the central pressures. To the best of our knowledge, only a single study was based on the CMR and tonometry measurements [6]. However in this latter study, a simplified area-based model was used for the evaluation of MWS on small groups of normal subjects and patients with dilated cardiomyopathy.

While the 2D thickness measurement is impaired, because of longitudinal curvature and of the partial volume effect present in the commonly acquired MR slices (8mm thickness), the 3D model is more accurate, especially in the apical region (figure 2) since it considers the LV longitudinal curvature (figure 1.B). In addition, because of the concentric and homogeneous nature of the LV adaptation in the studied population, the local values of the MWS calculated in the present study were averaged for the whole myocardium resulting in a global measure of MWS. However, this localized evaluation could be a valuable tool for the evaluation of heterogeneous myocardial alterations.

Usually, the geometrical factor is always combined with the LV pressure resulting in systolic MWS. In this study, the analysis of the LV geometrical factor variations according to aging and to an abnormal increase in afterload (AVS) indicated that this parameter can be used for the evaluation of LV remodeling in addition to the already established parameter M/EDV and to the parameter M/ESV. The decrease in this factor reflected the ability of the LV to adapt to an elevated pressure. Indeed, it contributed to the normalization of LV MWS with aging but also with less severe AVS (AVA-BSA > 0.45 cm^2/m^2). However, it remained unchanged in patients with severe AVS (AVA-BSA < 0.45 cm^2/m^2), indicating the inability of the LV to adapt to a substantial increase in systolic load. An additional analysis of delayed enhancement images of the severe AVS group revealed the presence of myocardial fibrosis in 8/12 patients. Our results indicated that the inability of the LV to adapt in this group might be strongly related to the presence of myocardial fibrosis. Therefore, as previously investigated [7], the value of surgery in our severe AVS subjects is questionable.

A methodological limitation consisted in the calculation of geometrical characteristics from adjacent slices separated by an inter-slice gap of 1 mm. This distance added to the slice thickness of 8 mm reduces the accuracy of the 3D correction. The reduction of the inter-slice distance may overcome this limitation. Another limitation is that, ideally, the healthy volunteers from the C2 group should be paired in age and sex with the AVS patients. Despite these limitations, our MWS estimate was shown to be sensitive enough to characterize variations in LV geometry related to aging or to the increase in afterload. Therefore, this parameter, which can be easily integrated to the MR evaluation of the LV function, should be taken into account for an accurate characterization of the LV adaptation to changes in systolic pressures load.

References

[1] Kass DA. Age-related changes in venticular-arterial coupling: pathophysiologic implications. Heart Fail Rev 2002; 7(1):51-62.

[2] Chen CH, Nakayama M, Nevo E, Fetics BJ, Maughan WL, Kass DA. Coupled systolic-ventricular and vascular stiffening with age: implications for pressure regulation and cardiac reserve in the elderly. J Am Coll Cardiol 1998; 32(5):1221-1227.

[3] Van Bortel LM, Balkestein EJ, van der Heijden-Spek JJ,Vanmolkot FH, Staessen JA, Kragten JA, Vredeveld JW, Safar ME, Struijker Boudier HA, Hoeks AP. Non-invasive assessment of local arterial pulse pressure: comparison of applanation tonometry and echo-tracking. J Hypertens 2001; 19(6):1037-1044.

[4] Malyar NM, Schlosser T, Buck T, et al. Using cardiac magnetic resonance tomography for assessment of aortic valve area in aortic valve stenosis. Herz 2006; 31(7):650-657.

[5] Grossman W, Jones D, McLaurin LP. Wall stress and patterns of hypertrophy in the human left ventricle. J Clin Invest 1975; 56(1):56-64.

[6] Fujita N, Duerinekx AJ, Higgins CB. Variation in left ventricular regional wall stress with cine magnetic resonance imaging: normal subjects versus dilated cardiomyopathy. Am Heart J 1993; 125(5):1337-1345.

[7] Carabello BA. Is it ever too late to operate on the patients with valvular heart disease? J Am Coll Cardiol 2004;44(2):376-383.

Address for correspondence.

Nadjia Kachenoura, PhD,
U678, 91 bd de l'Hôpital, Paris, France
nadjia.kachenoura@gmail.com